View metadata, citation and similar papers at core.ac.uk
brought to you by CORE
provided by Xiamen University Institutional Repository

29 卷 9 期 结 构 化 学 (*JIEGOU HUAXUE*) Vol. 29, No. 9
2010. 9 *Chinese J. Struct. Chem.* 1387~1393

Synthesis, Crystal Structure, Vibrational Spectroscopy, and Thermal Behavior of $Y[B_2O_3(OH)]_3$①

SUN Hua-Yu ZHOU Yan
HUANG Ya-Xi SUN Wei MI Jin-Xiao②
(*Department of Materials Science and Engineering, College of Materials, Xiamen University, Xiamen* 361005, *China*)

ABSTRACT The hydroxy yttrium hexaborate, $Y[B_2O_3(OH)]_3$, has been synthesized under mild hydrothermal conditions at 458 K. The crystal structure was solved and refined from single-crystal X-ray diffraction. It adopts a trigonal space group *R*3*c* (No. 161) with $a = 8.3942(4)$, $c = 20.6484(12)$ Å, $V = 1260.03(12)$ Å^3, $YB_6H_3O_{12}$, $M_r = 348.79$, $Z = 6$, $D_c = 2.758$ g/cm^3, $F(000) = 1008$, $\mu = 7.015$ mm^{-1}, $R = 0.0321$ and $wR = 0.0772$. Its crystal structure is made up of six-membered rings, alternating three-connected $[BO_3(OH)]$ tetrahedra and planar $[BO_3]$ trigonal groups, which are interconnected with each other by sharing their common oxygen corners to form a three-dimensional framework structure with six-membered ring channels that are occupied by the yttrium atoms and run along the *c* axis. FT-IR, Raman, and TG-DTA results are also presented.

Keywords: hydroxy yttrium borate, crystal structure, vibrational spectroscopy, thermal analysis

1 INTRODUCTION

In the past decades, much attention has been paid to rare earth borates due to their potential applications in laser host, nonlinear optical, luminescent and birefringent materials[1~4]. Exploiting novel complex borates with rare earth elements have been motivated and strengthened under the ever-growing demand in technology for new materials[5]. High-temperature reaction method is the most commonly used technique for preparing borates, but often fails for the synthesis of polyborate systems[6]. One possible approach for obtaining rare earth polyborates is to carry out the reaction at low temperature in a controlled manner[7]. And the hydrothermal method has been found to be an effective way to synthesize new hydrated rare earth polyborates. Li *et al*. using the molten boric acid synthesis method[7] and Belokoneva *et al*. using the hydrothermal synthesis method[8] have successfully synthesized $Ln[B_2O_3(OH)]_3$ (*Ln* = Sm-Lu). However, both two studies[7, 8] did not include yttrium which has quite similar properties with heavy rare earth elements. To the best of our knowledge, no hydrated yttrium borates are reported up to now. There are only several yttrium borates available, *i.e.* Y_3BO_6 and the modifications of YBO_3, in the Y_2O_3-B_2O_3 system[1, 3, 9~11]. In order to fully understand the crystal chemistry of the hydrated yttrium borates, we focus on the Y_2O_3-B_2O_3-H_2O system and prepared a new yttrium borate compound, $Y[B_2O_3(OH)]_3$, *via* a hydrothermal route. Here we report the synthesis and characterization of $Y[B_2O_3(OH)]_3$.

Received 24 November 2009; accepted 2 April 2010 (**ICSD 421260**)
① Supported by the National Natural Science Foundation of China (No. 40972035)
② Corresponding author. Fax: +86-592-2183937, E-mail: jxmi@xmu.edu.cn

2 EXPERIMENTAL

2. 1 Synthesis of $Y[B_2O_3(OH)]_3$

The title compound $Y[B_2O_3(OH)]_3$ was hydrothermally synthesized from a mixture of Y_2O_3, H_3BO_3 and deionized water. In a typical synthesis route, Y_2O_3 (0.307 g), H_3BO_3 (3.090 g) and 4 mL H_2O with the molar ratio of Y:B = 1:19 were mixed by stirring, then transferred to 20 mL Teflon-lined stainless steel autoclaves with filling degree of ~20%, and kept at 458 K for about 4 days under autogenous pressure. After heat treatment, the autoclaves were directly taken out of the oven, and cooled down to room temperature in air. Transparent, colorless *pseudo*-cube crystals with a yield of about 94% (based on yttrium element) was separated from the solution by filtration, washed with distilled water, and dried at room temperature. The powder X-ray diffraction (PXRD) pattern from experiment is well fitted with the calculated one based on the single-crystal structure, which indicates the purity of the sample. Systematic investigation on the experimental conditions shows that pure powder products of $Y[B_2O_3(OH)]_3$ can be obtained by optimizing the Y:B molar ratio and filling degree. However, large crystals suitable for single-crystal X-ray diffraction are preferential to grow under the condition of adding a small amount of NaF as mineralizer.

2. 2 Characterization

Several techniques were applied to characterize the title compound. The morphology of crystals was observed under a XL30 ESEM-TMP scanning electron microscope (SEM) operating at 20 kV. Fourier-Transform Infrared (FT-IR) spectrum was recorded from a powder sample palletized with KBr on an Avatar 360 series FT-IR Spectrometer (Nicolet) over a range of 400～4000 cm^{-1}, and Raman spectrum on a Renishaw 1000 Raman spectrometer over a 100～1200 cm^{-1} range. Powder X-ray diffraction (PXRD) histograms were taken using a Philips X'Pert-PRO diffractometer with Cu$K\alpha$ radiation (λ = 1.54056 Å). Thermal investigations were performed on a NETZSCH STA 409 PC/PG Thermo-Gravime- tric/ Differential Thermal Analyzer (TG-DTA) in Ar atmosphere with a heating rate of 10 K/min.

2. 3 Structure determination

A colorless *pseudo*-cube crystal of $Y[B_2O_3(OH)]_3$ (0.04mm × 0.04mm × 0.03mm) was carefully selected and checked under polarization microscope, and then mounted on a Rigaku R-AXIS RAPID image plate diffractometer equipped with a graphite-monochromatic Mo$K\alpha$ radiation (λ = 0.71073 Å, 50 KV/40mA) at 295(2) K. The single-crystal diffraction data were collected in the range of $3.43 \leq \theta \leq 27.37°$ and absorption correction was applied based on symmetry-equivalent reflections using the ABSOR program[12]. A total of 3720 reflections were measured, of which 649 (R_{int} = 0.0535) were independent, and 603 observed reflections with $I > 2\sigma(I)$ were used in structure analysis. The crystal structure of $Y[B_2O_3(OH)]_3$ was solved in space group $R3c$ (No. 161) with a = 8.3942(4) and c = 20.6484(12) Å by direct methods and refined by full-matrix least-squares refinement (SHELX-97)[13]. After the localization of yttrium, boron and some oxygen positions, the missing non-hydrogen atom sites were taken from difference Fourier maps. After the anisotropic displacement parameters had been included in the refinement, the hydrogen atom positions were located from difference Fourier maps without refinement. The final R = 0.0321, wR = 0.0772 ($w = 1/[\sigma^2(F_o^2) + (0.0395P)^2 + 3.8454P]$, where $P = (F_o^2 + 2F_c^2)/3$), S = 1.000, $(\Delta/\sigma)_{max}$ = 0.001, $(\Delta\rho)_{max}$ = 0.425 and $(\Delta\rho)_{min}$ = –0.397 e/Å^3. The flack factor is 0.011(18). The selected bond lengths and bond angles are listed in Table 1.

Table 1. Selected Bond Distances (Å) and Bond Angles (°) for $Y[B_2O_3(OH)]_3$

Bond	Dist.	Bond	Dist.
Y(1)–O(1)^{i} (×3)	2.465(3)	O(4)–B(1)–O(1)^{iii}	123.8(4)
Y(1)–O(2)^{i} (×3)	2.340(3)	O(4)–B(1)–O(3)^{ii}	119.3(4)
Y(1)–O(3)^{ii} (×3)	2.350(3)	O(1)^{iii}–B(1)–O(3)^{ii}	116.9(4)

B(1)–O(4)	1.373(6)	O(2)^{iv}–B(2)–O(1)^{ii}		112.2(4)		
B(1)–O(1)^{iii}	1.367(6)	O(2)^{iv}–B(2)–O(4)		112.0(4)		
B(1)–O(3)^{ii}	1.391(6)	O(1)^{ii}–B(2)–O(4)		111.7(4)		
B(2)–O(2)^{iv}	1.451(6)	O(2)^{iv}–B(2)–O(3)		111.5(4)		
B(2)–O(1)^{ii}	1.465(6)	O(1)^{ii}–B(2)–O(3)		101.0(4)		
B(2)–O(4)	1.469(6)	O(4)–B(2)–O(3)		107.8(3)		
B(2)–O(3)	1.515(5)	B(1)^{v}–O(1)–B(2)^{i}		132.1(4)		
B(1)–B(2)	2.470(9)	B(1)^{i}–O(3)–B(2)		123.9(4)		
B(1)^{i}–B(2)	2.565(9)	B(1)–O(4)–B(2)		120.8(4)		
B(1)–B(2)^{viii}	2.589(9)	D–H···A	D–H	H···A	D···A	D–H···A
		O(2)–H(1)···O(4)^{ix}	0.92	1.95	2.786(5)	151.8(2)

Symmetry codes: (i) $-x+y, -x+1, z$; (ii) $-y+1, x-y+1, z$; (iii) $-y+4/3, -x+2/3, z+1/6$; (iv) $-x+y-2/3, y-1/3, z+1/6$; (v) $-y+2/3, -x+4/3, z-1/6$; (vi) $-x+y-1/3, y+1/3, z-1/6$; (vii) $-y+1, x-y+1, z$; (viii) $x+1/3, x-y+2/3, z+1/6$; (ix) $-y+1/3, x-y+2/3, z-1/3$

3 RESULTS AND DISCUSSION

3.1 Structure description

The title compound $Y[B_2O_3(OH)]_3$ is isostructural to its analogs, $Ln[B_2O_3(OH)]_3$ (Ln = Sm-Lu)[7, 8] (see Fig. 1). There are two crystallographically different boron sites in the structure. B(1) is coordinated with three neighboring oxygen atoms to form a planar $[BO_3]$ group, and B(2) with four oxygen atoms to yield a tetrahedral $[BO_3(OH)]$ group. Each planar $[BO_3]$ group links to three tetrahedral $[BO_3(OH)]$ groups *via* common oxygen vertices, *vice versa* for the tetrahedral $[BO_3(OH)]$ groups (see Fig. 1a, b)[14]. The overall crystal structure is made from six-membered ring borates, $\{[B_2O_4(OH)]_3\}^{9-}$, interconnected with each other to form a three-dimensional framework structure. The anionic part of the structure consists of a six-membered ring of $\{[B_2O_4(OH)]_3\}^{9-}$ as a fundamental building block (FBB), which is constituted by three $[BO_3]$ groups (triangular boron: △) and three $[BO_3(OH)]$ groups (tetrahedral boron: □) alternately (see Fig. 2a). It can be written as FBB6:3△+3□ with the help of the conception of FBBs after Christ and Clark[15], Burns *et al.*[16]. A similar FBB6:3△+3□ can be observed in the structure of $Na_3VB_6O_{13}$[17], which can be envisaged as the condensation of three OH-terminals of $[BO_3(OH)]$ tetrahedra and fusing into a common oxygen atom (see Fig. 2b). Topologically, the structure can be considered as being stacked from a cubic close-packed array of the motifs of FBB6:3△+3□ along the *c* axis (see Fig. 2c). Yttrium atoms occupy half amount of 'tetrahedral interstice' surrounded by four six-membered rings (FBB6:3△+3□). The six-membered rings develop into channels with ditrigonal section along the *c* axis (Fig.1) whose centers are occupied by Y atoms. Each yttrium atom is surrounded by nine oxygen atoms, with Y–O distances ranging from 2.340(3) to 2.465(3) Å, which is similar to the Y–O distances (2.45 Å) in $Y_3Al_5O_{12}$[18] (see Fig. 2c). For the trigonal $[BO_3]$ group, the B–O bond lengths and O–B–O bond angles of $Y[B_2O_3(OH)]_3$ are in the ranges of 1.367(6)～1.391(6) Å and 116.9(4) ～ 123.8(4)º, while 1.451(6)～1.515(6) Å and 101.0(4)～112.2(4)º for the $[BO_3(OH)]$ tetrahedron, which are in good agreement with those reported previously in counterparts[7, 8]. And the atoms' distances of B(1)···B(2) (*i.e.* 2.470, 2.565 and 2.589 Å) in $Y[B_2O_3(OH)]_3$ are also similar with its analogs (Ho and Gd)[7, 8].

It has been noticed that the cell of $Y[B_2O_3(OH)]_3$ (a = 8.3942(4), c = 20.6484(12) Å, γ = 120°) can be transformed into a rhombohedral cell of $a = b = c$ = 8.4179 Å and $\alpha = \beta = \gamma$ = 59.814° by a matrix of (1/3, –1/3, –1/3; –2/3, –1/3, –1/3; 1/3, 2/3, –1/3). And the interaxial angles in the new rhombohedral cell are quite close to 60°. Thus this new cell can be further transformed into a *pseudo*-cubic face-centre cell of $a = b = c$ = 11.8880 Å and $\alpha = \beta = \gamma$ = 89.839° by a matrix of (1, –1, 1; 1, 1, –1; –1, 1, 1). This is why the motifs of six-membered rings (FBB6:3△+3□) display *pseudo*-cubic face-centre arrays and $Y[B_2O_3(OH)]_3$ has the morphology of *pseudo*-cube.

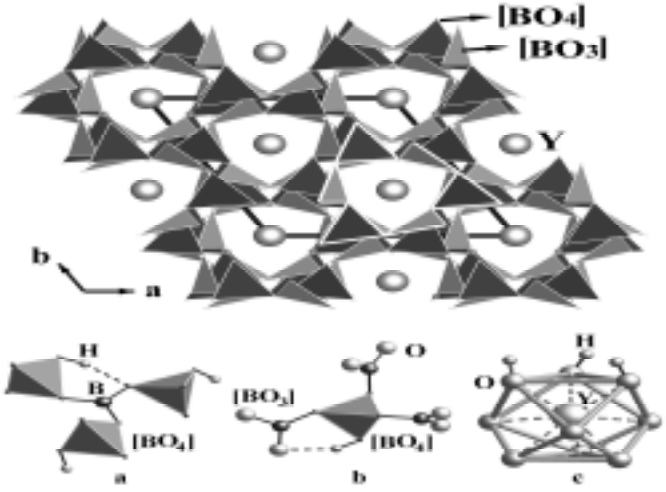

Fig. 1. Crystal structure of $Y[B_2O_3(OH)]_3$ viewed along the *c* axis. (a) Linkage of $[BO_3]$; (b) Linkage of $[BO_4]$; (c) Coordination environment of yttrium ($[BO_4]$ tetrahedra: dark grey, $[BO_3]$ trigonal planar: light grey)

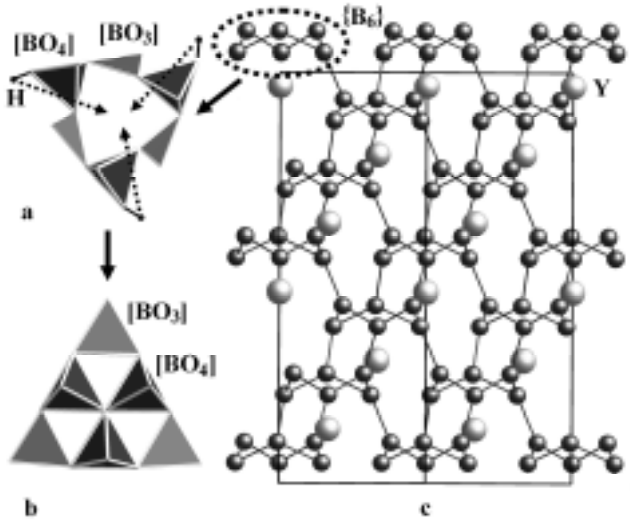

Fig. 2. (a) Fundamental building block (FBB6:3△+3□) of six-membered ring $\{[B_2O_4(OH)]_3\}^{9-}$ in the crystal structure of $Y[B_2O_3(OH)]_3$ compared with (b) a similar FBB6:3△+3□ in the crystal structure of $Na_3VB_6O_{13}$; (c) topological chart, with oxygen atoms being removed for clarity

3. 2 Vibrational spectroscopy

Although Li *et al.*[2] and Belokoneva *et al.*[3] have respectively characterized the compounds of $Ln[B_2O_3(OH)]_3$ (*Ln* = Sm-Lu) in various aspects, little attention was paid to the characterization of FT-IR and Raman. Only the FT-IR of $Ho[B_2O_3(OH)]_3$ was reported in the relative system. Here the FT-IR and Raman spectra of $Y[B_2O_3(OH)]_3$ are presented in Fig. 3. The FT-IR bands of $Y[B_2O_3(OH)]_3$ are significantly different from its Ho counterpart in intensities and frequencies. The most probable assignments are given in Table 2 by referring to a relative literature[19]. An intense broad band at 3368 cm^{-1} with a shoulder at 3431 cm^{-1} can be ambiguously attributed to the stretching vibrations of O–H bonds. The band at 1632 cm^{-1} can also be assigned to the characteristic vibrations of O–H. The bands of 1110～740 cm^{-1} in FT-IR and Raman spectra mainly resulted from the stretching vibrations of B–O and B–O–B bonds of condensed $[BO_3]$ and $[BO_4]$ anions. The bands in the range of 740～500 cm^{-1} are relative to the deformation vibrations of $[BO_3]$ and $[BO_4]$ anions. The frequencies of Raman spectra less than 350 cm^{-1} may be attributed to the lattice vibration.

Table 2. Observed Infrared Frequencies/Raman Shifts (cm^{-1}) and Band Assignments for $Y[B_2O_3(OH)]_3$

IR frequencies (cm^{-1})	Raman shifts (cm^{-1})	Possible assignments
3431(sb), 3368(sb)		O–H Stretching
1632(m)		H–O–H bending
1381(mb)		Asymmetric stretching of B{3}–O*
1242(m)		In-plane bending of B–O–H
1085(w), 1047(m),	1097(wb), 1045(wb)	Asymmetric stretching of B{4}–O
921(w)	912(w)	Symmetric stretching of B{3}–O
880(w)	829(m), 750(m)	Symmetric stretching of B{4}–O
735(w), 672(w)	687(s)	Out-of-plane bending of B{3}–O
	647(s), 612(w),	Symmetric pulse vibration of hexaborate anion
565(w)	553(w), 526(s)	Bending of B{3}–O and B{4}–O
		O–B–O terminal bending
	414(w), 381(s)	Bending of B{4}–O
	349(w), 330(w), 286(m), 242(w), 212(w), 177(m), 144(w), 120(m)	Lattice vibration

* B{3} denotes the planar coordination and B{4} the tetrahedral coordination.

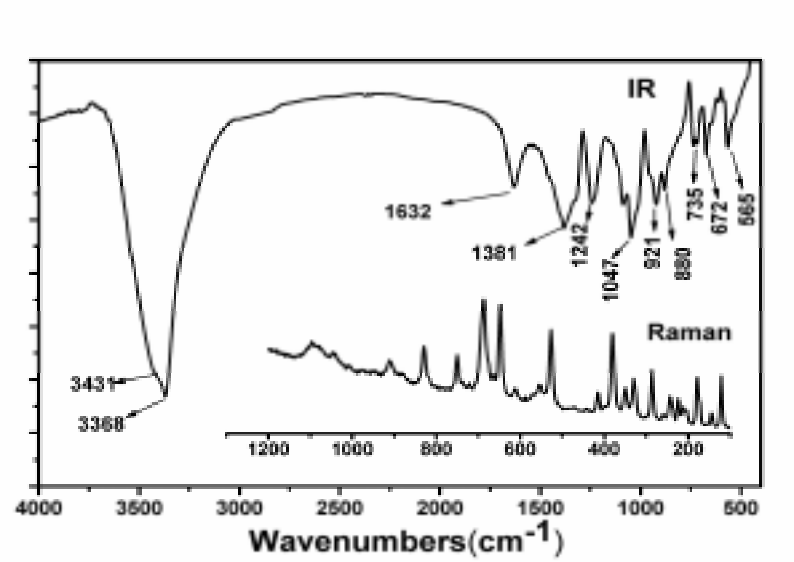

Fig. 3. Fourier-transform infrared (FT-IR) and Raman spectra of $Y[B_2O_3(OH)]_3$

3. 3 Thermal behavior

The thermal stability of the title compound has been investigated. There is a sharp endothermic peak observed at 681 °C in the DTA curve, which corresponds to a weight loss of 8.44% occurring in the range of 520～720 °C in the TG curve (Fig. 4). This weight loss is attributed to the dehydration of hydroxyls of $Y[B_2O_3(OH)]_3$ during decomposition; it is in agreement with the theoretical value (calcd.: 7.75%) for the loss of 1.5 water molecule of $Y[B_2O_3(OH)]_3$. The present DTA curve of $Y[B_2O_3(OH)]_3$ is significantly different from that of $Gd[B_2O_3(OH)]_3$ given by Li *et al.* (2002). The previously reported work shows that products of $Ln[B_2O_3(OH)]_3$ after decomposition crystallizes in two different types of phases. One is to form pentaborates LnB_5O_9 (Ln = Sm-Ho) for rare earths with larger ionic radii, and the other to directly yield orthoborate $LnBO_3$ (*Ln* = Yb-Lu) for rare earths with smaller ionic radii. The products of Er and Tm, which lie in the interval between the above given ranges, are the mixture of both LnB_5O_9 and $LnBO_3$. Powder X-ray diffraction analysis indicates that the title compound does not follow the above rule. As shown in Fig. 5, a new intermediate phase was observed in the gap of temperatures between the decomposition of $Y[B_2O_3(OH)]_3$ and the formation of YBO_3. The composition of the intermediate phase is not clear and needs further investigation.

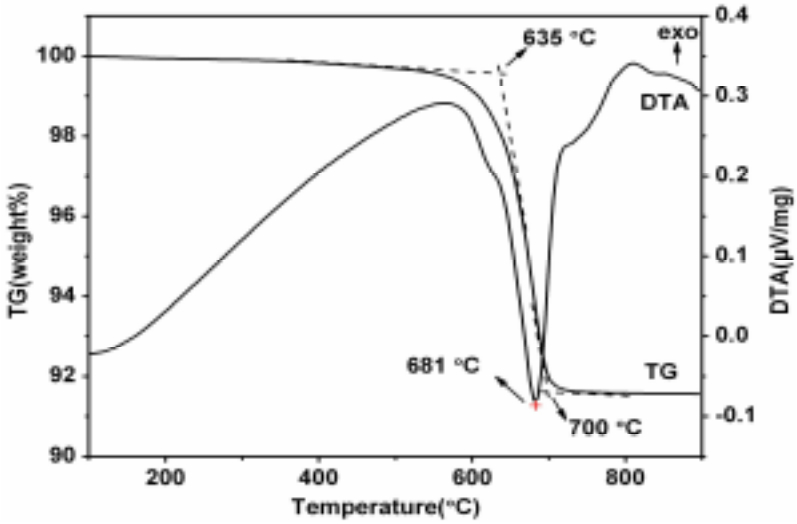

Fig. 4. TG-DTA curves of $Y[B_2O_3(OH)]_3$

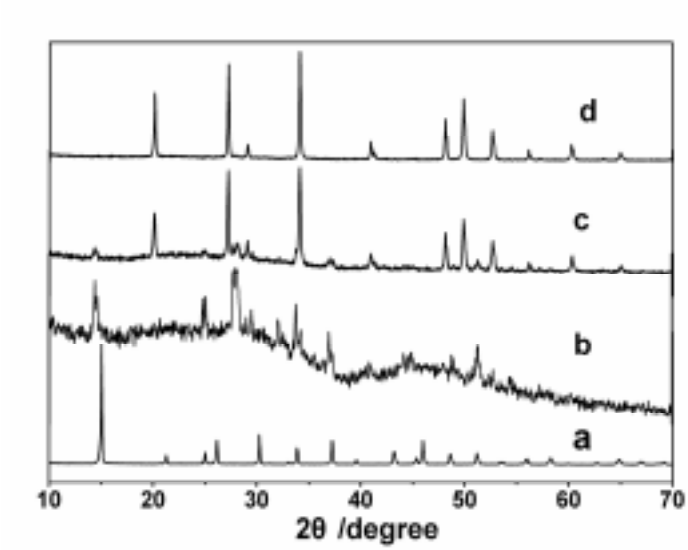

Fig. 5. Powder X-ray diffraction patterns of $Y[B_2O_3(OH)]_3$ before and after heat treatment at different temperatures. (a) Without heat treatment; (b～d) After heat treatment by being kept for 3 h at 650 °C (b), 670 °C (c) and 700 °C (d), respectively. Phases: (a) $Y[B_2O_3(OH)]_3$, (b) An unknown intermediate compound, (c) The mixture of (b) and (d), (d) YBO_3

4 CONCLUSION

In summary, the synthesis, crystal structure, vibrational spectroscopy, and thermal properties of the hydrated yttrium borate $Y[B_2O_3(OH)]_3$ are present in this work. The structure contains a six-membered ring $\{[B_2O_3(OH)]_3\}^{9-}$, constructed from alternating three $[BO_3(OH)]$ tetrahedra and three $[BO_3]$ trigonal planar, as a fundamental building block. The fundamental building blocks are arrayed in a motif of *pseudo*-cubic close packing topologically, leading to a *pseudo*-cubic face-centre cell and a morphology of *pseudo*-cube. Compared with its isotypic Ho-analogs, $Y[B_2O_3(OH)]_3$ has different vibrational and thermal behaviors. In addition, the hydrothermal approach has also been proved to be an efficient route in extending varieties of rare earth polyborates.

ACKNOWLEDGEMENTS

The authors are grateful to Dr. Dong-Ping Lv for TG-DTA measurement and Dr. Sheng-Zhi Hu for his valuable help.

REFERENCES

(1) Chadeyron, G.; Mahiou, R.; ElGhozzi, M.; Arbus, A.; Zambon, D.; Cousseins, J. C. *J. Lumin.* **1997**, 72–74, 564–566.

(2) Ye, Q.; Shah, L.; Eichenholz, J.; Hammons, D.; Peale, R.; Richardson, M.; Chin, A.; Chai, B. H. T. *Opt. Commun.* **1999**, 164, 33–37.

(3) Lin, J. H.; Zhou, S.; Yang, L. Q.; Yao, G. Q.; Su, M. Z.; You, L. P. *J. Solid State Chem.* **1997**, 134, 158–163.

(4) Yang, Z.; Ren, M.; Lin, J. H.; Su, M. Z.; Tao, Y.; Wang, W. *Chem. J. Chinese U.* **2000**, 21, 1339–1343.

(5) Lin, J. H.; Wang, Y. X.; Li, L. Y. *Inorg. Chem. Focus II, Wiley–VCH: Weinheim, Germany* **2005**, 293–317.

(6) Leonyuk, N. I. *J. Cryst. Growth* **1997**, 174, 301–307.

(7) Li, L. Y.; Lu, P. C.; Wang, Y. Y.; Jin, X. L.; Li, G. B.; Wang, Y. X.; You, L. P.; Lin, J. H. *Chem. Mater.* **2002**, 14, 4963–4968.

(8) Belokoneva, E. L.; Ivanova, A. G.; Stefanovich, S. Y.; Dimitrova, O. V.; Kurazhkovskaya, V. S. *Crystallogr. Rep.* **2004**, 49, 603–613.

(9) Chadeyron, G.; ElGhozzi, M.; Mahiou, R.; Arbus, A.; Cousseins, J. C. *J. Solid State Chem.* **1997**, 128, 261–266.

(10) Boyer, D.; Bertrand-Chadeyron, G.; Mahiou, R.; Brioude, A.; Mugnier, J. *Opt. Mater.* **2003**, 24, 35–41.

(11) Zargarova, M. I.; Kuli-zade, E. S. *Russ. J. Inorg. Chem. (Engl. Transl.)* **1998**, 43, 612–614.

(12) Higashi, T. *ABSCOR, Empirical Absorption Based on Fourier Series Approximation*; Rigaku Corporation: Tokyo **2007**.

(13) Sheldrick, G. M. *SHELXS97 and SHELXL97[CP]*, University of Göttingen, Göttingen **1997**.

(14) Brandenburg, K. *DIAMOND V3.2. Crystal Impact GbR*, Bonn **1997–2009** Germany.

(15) Christ, C. L.; Clark, J. R. *Phys. Chem. Miner.* **1977**, 2, 59–87.

(16) Burns, P. C.; Grice, J. D.; Hawthorne, F. C. *Can. Mineral.* **1995**, 33, 1131–1151.

(17) Touboul, M.; Penin, N.; Nowogrocki, G. *J. Solid State Chem.* **2000**, 150, 342–346.

(18) Mary, S. S.; Kirupavathy, S. S.; Mythili, R.; Gopalakrishnan, R. *Spectrochim. Acta A* **2008**, 71, 1311–1316.

(19) Li, J.; Xia, S. P.; Gao, S. Y. *Spectrochim. Acta A* **1995**, 51, 519–532.